ChemComm

COMMUNICATION

View Article Online
View Journal | View Issue

Cite this: *Chem. Commun.*, 2014, **50**, 12564

Received 23rd May 2014,
Accepted 17th August 2014

DOI: 10.1039/c4cc03973d

www.rsc.org/chemcomm

Understanding $Na_2Ti_3O_7$ as an ultra-low voltage anode material for a Na-ion battery†

Jing Xu,[a] Chuze Ma,[a] Mahalingam Balasubramanian[b] and Ying Shirley Meng*[a]

An in-depth understanding of $Na_2Ti_3O_7$ as a Na-ion battery anode is reported. The battery performance is enhanced by carbon coating, due to increased electronic conductivity and reduced solid electrolyte interphase formation. Ti^{4+} reduction upon discharge is demonstrated using *in situ* XAS. The self-relaxation behaviour of the fully intercalated phase is revealed.

Na-ion batteries have recently gained increased recognition as intriguing candidates for next-generation large-scale energy storage systems, stemming from the natural abundance and broad distribution of Na resources. Although the energy density of Na-ion batteries is not as high as that of Li-ion batteries, which is one of the most dominating energy technologies in this decade, Na-ion batteries operating at room temperature can be suitable for applications where specific volumetric and gravimetric energy density requirements are not as stringent as in EVs, namely in electrical grid storage of intermittent energy produced *via* renewable sources.[1] This would also contribute to a significant reduction in the costs connected to the use of renewable sources, making Na-ion technology complementary to Li-ion batteries for stationary storage.[2,3]

For the past several years, it has been realized that because the Na ion has a larger ionic radius than the Li ion, materials with an open framework are preferred for facile Na ion insertion/extraction. Following this strategy, many breakthroughs in cathode materials such as layered and polyanion compounds have been achieved.[4] However, the development of suitable anode materials for Na-ion batteries remains a considerable challenge.[5] Graphite cannot be used as the anode, since it is unable to accommodate Na ion reversibly.[6,7] Hard carbon is shown to insert and de-insert Na ions; however, the reversibility still requires further improvement.[7–9] Na-alloys have been proposed as possible alternatives, as they can potentially provide higher specific capacities.[10] These alloys, however, suffer from large volume changes upon uptake/removal of Na, in analogy to Li-alloys.[3] Another emerging class of materials is that of transition metal oxides. For example, $NaVO_2$ is shown to yield a reversible capacity, but its operating voltage is 1.5 V *vs.* Na^+/Na, leading to a low energy density.[11] Ti-based oxides are suggested to be an attractive alternative, considering that $Li_4Ti_5O_{12}$ is one of the few commercialized anode materials used in a Li-ion battery.[12] Several different sodium titanates have been explored as anodes for use in a Na-ion battery.[13–15] Among them, a study by Palacín *et al.* demonstrated that layered oxide $Na_2Ti_3O_7$ could reversibly exchange Na ions to provide the lowest voltage ever reported for an oxide insertion electrode.[14] The ultra-low voltage and intrinsic high reversibility of this material make it a strong anode candidate for use in a Na-ion battery. Very recently, the same group identified the fully intercalated phase, $Na_4Ti_3O_7$, and provided additional insight into the low intercalation potential, using DFT calculations.[15] However, more work is still required to closely connect the fundamental properties with the battery performance and to systematically evaluate whether it can be a viable anode for a Na-ion battery. Herein, we report a comprehensive study to unveil the underlying relationship between the intercalation mechanism and battery performance for the $Na_2Ti_3O_7$ anode.

$Na_2Ti_3O_7$ was prepared by a mechanical mixing of anatase TiO_2 and anhydrous Na_2CO_3, followed by calcination at 800 °C (for Experimental details, see the ESI†). The as-synthesized material was well crystallized in the $P21/m$ space and adopted a pellet shape (Fig. S1, ESI†). The white color of the obtained powder suggests its intrinsic insulating property, which is undesired for battery applications. So carbon coating by sucrose pyrolysis was applied to improve the electronic conductivity.[16] Thermogravimetric analysis suggests that the coated material contains 9% carbon (Fig. S2, ESI†). The electrochemical properties were tested in a Na half cell over a voltage window of 0.01–2.5 V. Fig. S3 (ESI†) presents the first cycle electrochemical profile. The average intercalation potential is around 0.35 V, and a large amount of excess capacity in the first discharge is observed mainly due to

[a] *Department of NanoEngineering, University of California San Diego, 9500 Gilman Drive, La Jolla, CA 92093, USA. E-mail: shirleymeng@ucsd.edu*
[b] *X-ray Science Division, Advanced Photon Source, Argonne National Laboratory, 9700 South Cass Avenue, Argonne, Illinois 60439, USA*

† Electronic supplementary information (ESI) available. See DOI: 10.1039/c4cc03973d

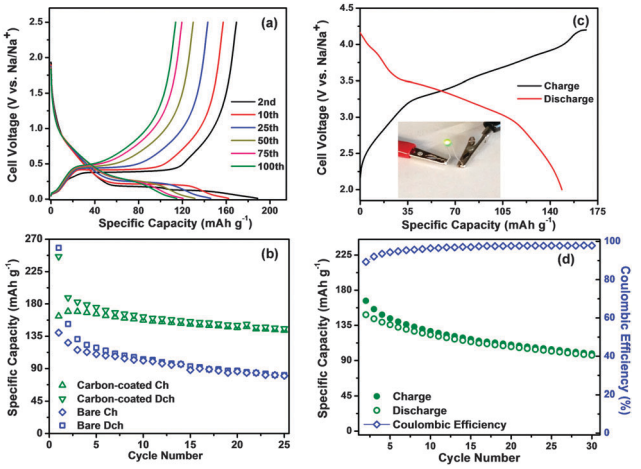

Fig. 1 (a) Voltage profiles of carbon-coated $Na_2Ti_3O_7$ in the 2nd, 10th, 25th, 50th, 75th and 100th cycles at C/10 rate. (b) Cycling performance for carbon-coated and bare $Na_2Ti_3O_7$. (c) Voltage profiles and (d) Cycling performance for the Na full cell (the specific capacity is calculated based on anode materials).

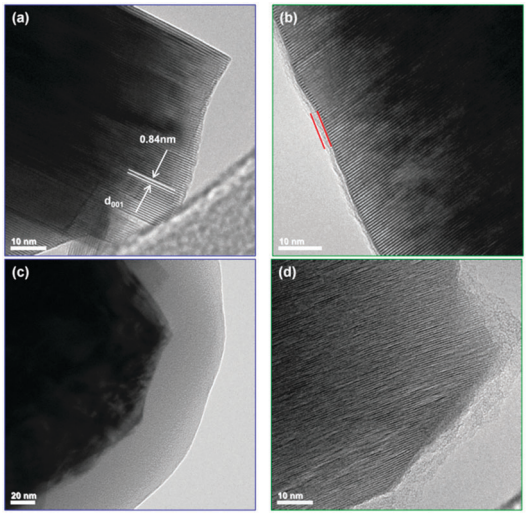

Fig. 2 TEM images for (a) bare and (b) carbon-coated $Na_2Ti_3O_7$ at pristine state. TEM images for (c) bare and (d) carbon-coated $Na_2Ti_3O_7$ after 1st discharge.

irreversible Na intercalation into the carbon additive (Super P) in the electrode, consistent with previous literature.[14] Starting from the first charge, a theoretical capacity of 177 mA h g^{-1} (corresponding to 2 Na insertions per formula unit) is fully delivered and a capacity of more than 115 mA h g^{-1} is well maintained after 100 cycles for the carbon-coated $Na_2Ti_3O_7$ (Fig. 1a). Besides the excellent cycling properties, a good rate performance is achieved due to improved electronic conductivity (Fig. S4, ESI†). Compared with carbon-coated $Na_2Ti_3O_7$, the as-synthesized (henceforth referred to as "bare $Na_2Ti_3O_7$") displays notably reduced capacity (Fig. 1b). Therefore, the coated carbon plays an important role in enhancing the battery performance.

To evaluate the practical applications of $Na_2Ti_3O_7$, herein we demonstrate for the first time a full Na cell using $Na_2Ti_3O_7$ as the anode material. Fig. 1c shows the voltage profile of the $Na_2Ti_3O_7$/$Na_{0.80}Li_{0.12}Ni_{0.22}Mn_{0.66}O_2$ full cell, in which the cathode material, P2 – $Na_{0.80}Li_{0.12}Ni_{0.22}Mn_{0.66}O_2$, has been reported by us previously.[17] Due to the ultralow voltage of the $Na_2Ti_3O_7$ anode, the average voltage of this full cell is as high as 3.1 V, which is comparable to that of the commercial Li-ion battery. As seen in the Fig. 1c inset, the Na full cell can easily light up a 2.5 V LED bulb. The cycling of the full cell at a C/10 rate is displayed in Fig. 1d. The capacity is stabilized at 105 mA h g^{-1} after 25 cycles (the capacity is determined by the anode active material). At the same time, the coulombic efficiency is gradually increased to above 98% and maintained in the subsequent cycles. The overall energy density is 100 W h kg^{-1}, based on the total weight of active materials from both cathode and anode. Although the energy density is lower than that of the Li-ion battery, it should be noted that Na does not alloy with Al, so that the Al current collector can be used for both the cathode and the anode. This will help to further improve the energy density of the Na-ion battery and reduce the manufacturing cost.

High resolution transmission electron microscopy (HRTEM) images revealed the surface morphologies for bare and carbon-coated $Na_2Ti_3O_7$ samples. In the pristine state (Fig. 2a and b), the lattice fringes are clearly observed, implying good crystallinity. The width (0.84 nm) of the neighbouring fringe distance corresponds to the (001) plane. As suggested by Fig. 2b, the carbon is uniformly coated on the surface of $Na_2Ti_3O_7$ with a thickness of around 3 nm. After the 1st discharge, an amorphous layer with a thickness of 30–50 nm is seen on the bare $Na_2Ti_3O_7$ particle (Fig. 2c), indicating a severe side reaction at the solid electrolyte interface (SEI). In contrast, the SEI layer is largely inhibited in the carbon-coated $Na_2Ti_3O_7$ (Fig. 2d). Consequently, it is noticed that the initial coulombic efficiency is increased by 11% from the bare to the carbon-coated sample (Fig. S3, ESI†). This demonstrates that in addition to improving the electronic conductivity, the coated carbon on the surface could also serve as a protection layer to prohibit side reactions of the electrolyte and enhance battery performance. It should be noted that the carbon coating could only partially improve the inefficiency in the 1st cycle, since the main irreversible capacity results from Na reaction with super P.[14]

In order to understand the structural evolution and the ultra low voltage for $Na_2Ti_3O_7$ upon cycling, $Na_xTi_3O_7$ as well as its Li analogue $Li_xTi_3O_7$ ($2 \leq x \leq 4$) was investigated by first principles calculations. The fully intercalated phase, $Na_4Ti_3O_7$, is identified by our calculations, which is in agreement with those in Dr Palacín *et al.*'s recent report.[15] More details of the phase transformation can be revealed by closely examining structural differences between $Na_2Ti_3O_7$ and $Na_4Ti_3O_7$. As shown in Fig. 3a, although there is no bond broken in Ti–O frameworks, the Na sites experience drastic variations. The Na-ion coordination decreases from 9 and 7 in the pristine state to 6 after full intercalation. In addition, to accommodate more Na ions in the structure, the lattice parameters are adjusted by shearing the Ti–O slabs. The *c* lattice parameter is reduced due to a better screening effect from a high Na-ion concentration in the Na layer. More interestingly, the dramatic Na site change is not only due to the shift of the Ti–O slab but is also contributed by modifications within the Ti–O framework.

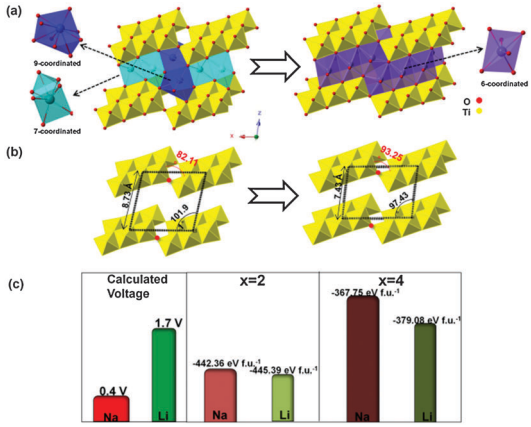

Fig. 3 (a) The phase transformation (b) related structural change upon Na intercalation. (c) The calculated voltage and electrostatic energy at $x = 2$ and $x = 4$ for $Li_xTi_3O_7$ and $Na_xTi_3O_7$ respectively. The narrow bar is for $Li_xTi_3O_7$ and wide one for $Na_xTi_3O_7$.

After full intercalation, the joint angle between neighbouring Ti–O blocks is enlarged from 82.11 to 93.25° (Fig. 3b). Therefore, it is fascinating to notice that this type of framework possesses structural flexibility to some degree, which is quite unique compared with traditional layered intercalation compounds, such as $LiCoO_2$. As for the intercalation voltage, the calculated values for both $Na_xTi_3O_7$ and $Li_xTi_3O_7$ are basically consistent with the experimental results[15] (Fig. 3c). Based on the Nernst equation, the battery voltage is directly related to the Gibbs free energy change during chemical reaction. Thus, the lower voltage for $Na_xTi_3O_7$ compared with $Li_xTi_3O_7$ is associated with the smaller change in Gibbs free energy in the Na case. In addition, we have studied the electrostatic interaction in the crystal structure using Ewald summation.[18] It is interesting to see that there is a bigger jump in the electrostatic energy for $Na_xTi_3O_7$ from $x = 2$ to $x = 4$ than that for $Li_xTi_3O_7$, demonstrating a much stronger electrostatic repulsion in $Na_4Ti_3O_7$. Such a large electrostatic repulsion leads to structural instability and consequently, increases the Gibbs free energy for $Na_4Ti_3O_7$. Therefore, the overall change in the Gibbs free energy upon intercalation is reduced in the Na case and the voltage is lowered accordingly.

Owing to the strong electrostatic repulsion in the fully discharged phase, $Na_4Ti_3O_7$, a "self-relaxation" behaviour was observed. As shown in Fig. 4a, the diffraction pattern for the $Na_4Ti_3O_7$ phase is obtained right after the full discharge is completed. However, for the electrodes stored in the glovebox for 3 and 10 days after the full discharge, the intensity of peaks from the $Na_4Ti_3O_7$ phase, such as (−302) and (104), gradually and systematically diminishes. Concomitantly, the diffraction peaks from the $Na_2Ti_3O_7$ phase increase steadily. These observations suggest that the $Na_4Ti_3O_7$ structure undergoes self-relaxation. This property has also been captured electrochemically. Fig. S5a and b (ESI†) compare the voltage profiles for $Na_2Ti_3O_7$ under cycling with and without interval rest (between charge and discharge) respectively. It is observed that the open circuit voltage for the cell with interval rest is increased gradually during the rest time, indicating the structural relaxation. Additionally, though the discharge performances are identical in the two cases, only the cell with interval rest can deliver 130 mA h g^{-1} capacity in the first charge and further decay is seen in the subsequent cycles (Fig. S5c and S6, ESI†). Considering that this self-relaxation in the anode material would lead to self-discharge in the actual full cell, it could be one of the main bottlenecks for using $Na_2Ti_3O_7$ as an anode for Na-ion batteries in practice.

The oxidation state of titanium was studied using *in-situ* X-ray absorption spectroscopy (XAS). Customized coin cells were used to prevent the sample contamination. As Ti^{3+} is extremely sensitive to oxidization ($Ti^{3+} \rightarrow Ti^{4+}$), *ex situ* characterization attempts to detect Ti reduction during the lithiation process were not successful. It is important to make sure that throughout the entire characterization process, the electrodes are never exposed to an ambient environment. In Fig. 4b, the Ti-K edge is gradually shifted towards the lower energy region from the pristine state to 0.01 V. The shape and position of the pre-edge as well as the position of the main edge for the fully discharged sample approach those found for Ti_2O_3, demonstrating that Ti^{4+} is reduced upon Na-ion intercalation. The decrease in the pre-edge peak is ascribed to the reduced hybridization between Ti-3d and O-2p orbitals during Ti ion reduction.[19,20] In fact, this Ti reduction is similar to its Li counterparts.[19,21] Therefore, it is speculated that the ultra-low voltage observed for $Na_2Ti_3O_7$ material during intercalation could mainly originate from the crystal structural perspective as discussed above, instead of electronic contributions.

In summary, a comprehensive study on $Na_2Ti_3O_7$ as an ultra-low voltage anode for Na-ion batteries is reported. Cyclability and coulombic efficiency are significantly enhanced with carbon coating due to increased electronic conductivity and reduced SEI formation. The Na full cell with a high operating voltage is demonstrated by taking advantage of the ultra-low voltage of the $Na_2Ti_3O_7$ anode. The self-relaxation behaviour for the fully intercalated phase, $Na_4Ti_3O_7$, is shown for the first time, which results from structural instability as suggested by first principles calculations. Ti^{4+}/Ti^{3+} is the active redox couple obtained upon cycling based on XANES characterization. These findings unravel the underlying relation between the unique properties and the battery performance of the $Na_2Ti_3O_7$ anode, which should ultimately shed light on possible strategies for future improvements.

Jing Xu and Chuze Ma contributed equally to this work. The authors are grateful for the financial support from the National

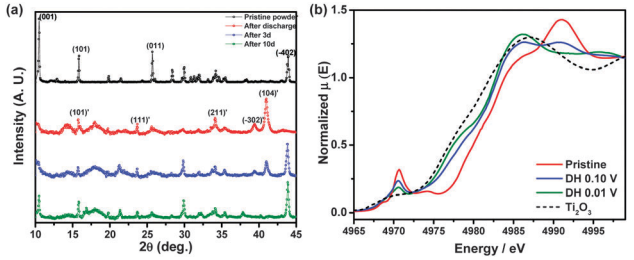

Fig. 4 (a) Change in the XRD patterns with time for fully discharged electrodes. (b) Normalized Ti K-edge XANES for $Na_2Ti_3O_7$ at pristine state (red), after discharged to 0.10 V (blue), and after discharged to 0.01 V (green).

Science Foundation under CAREER Award Number 1057170. The XAS work was performed at 20-BM-B at Argonne's Advanced Photon Source (APS); the APS is supported by the USDOE under contract No. DE-AC02-06CH11357. The authors appreciate the fruitful discussion and assistance from Dr Dae Hoe Lee and Mr James Somerville at the University of California San Diego.

Notes and references

1 B. L. Ellis and L. F. Nazar, *Curr. Opin. Solid State Mater. Sci.*, 2012, **16**, 168.
2 H. L. Pan, Y. S. Hu and L. Q. Chen, *Energy Environ. Sci.*, 2013, **6**, 2338; V. Palomares, M. Casas-Cabanas, E. Castillo-Martinez, M. H. Han and T. Rojo, *Energy Environ. Sci.*, 2013, **6**, 2312.
3 M. Valvo, F. Lindgren, U. Lafont, F. Bjorefors and K. Edstrom, *J. Power Sources*, 2014, **245**, 967.
4 J. Xu, D. H. Lee and Y. S. Meng, *Funct. Mater. Lett.*, 2013, **6**, 1330001; M. R. Palacín, *Chem. Soc. Rev.*, 2009, **38**, 2565.
5 K. Sung-Wook, S. Dong-Hwa, M. Xiaohua, G. Ceder and K. Kisuk, *Adv. Energy Mater.*, 2012, **2**, 710; M. D. Slater, D. Kim, E. Lee and C. S. Johnson, *Adv. Funct. Mater.*, 2012, 947.
6 G. E. Pascal and M. Fouletier, *Solid State Ionics*, 1988, **28**, 1172.
7 D. A. Stevens and J. R. Dahn, *J. Electrochem. Soc.*, 2001, **148**, A803.
8 D. A. Stevens and J. R. Dahn, *J. Electrochem. Soc.*, 2000, **147**, 1271; D. A. Stevens and J. R. Dahn, *J. Electrochem. Soc.*, 2000, **147**, 4428.
9 R. Alcantara, J. M. Jimenez-Mateos, P. Lavela and J. L. Tirado, *Electrochem. Commun.*, 2001, **3**, 639; S. Komaba, W. Murata, T. Ishikawa, N. Yabuuchi, T. Ozeki, T. Nakayama, A. Ogata, K. Gotoh and K. Fujiwara, *Adv. Funct. Mater.*, 2011, **21**, 3859.
10 A. Darwiche, C. Marino, M. T. Sougrati, B. Fraisse, L. Stievano and L. Monconduit, *J. Am. Chem. Soc.*, 2012, **134**, 20805; X. Yunhua, Z. Yujie, L. Yihang and W. Chunsheng, *Adv. Energy Mater.*, 2013, **3**, 128; L. Wu, P. Pei, R. J. Mao, F. Y. Wu, Y. Wu, J. F. Qian, Y. L. Cao, X. P. Ai and H. X. Yang, *Electrochim. Acta*, 2013, **87**, 41; M. Shimizu, H. Usui and H. Sakaguchi, *J. Power Sources*, 2014, **248**, 378.
11 C. Didier, M. Guignard, C. Denage, O. Szajwaj, S. Ito, I. Saadoune, J. Darriet and C. Delmas, *Electrochem. Solid-State Lett.*, 2011, **14**, A75.
12 E. Ferg, R. J. Gummow, A. Dekock and M. M. Thackeray, *J. Electrochem. Soc.*, 1994, **141**, L147; T. Ohzuku, A. Ueda and N. Yamamoto, *J. Electrochem. Soc.*, 1995, **142**, 1431.
13 M. Shirpour, J. Cabana and M. Doeff, *Energy Environ. Sci.*, 2013, **6**, 2538; H. Xiong, M. D. Slater, M. Balasubramanian, C. S. Johnson and T. Rajh, *J. Phys. Chem. Lett.*, 2011, **2**, 2560; A. Rudola, K. Saravanan, S. Devaraj, H. Gong and P. Balaya, *Chem. Commun.*, 2013, **49**, 7451.
14 P. Senguttuvan, G. Rousse, V. Seznec, J.-M. Tarascon and M. R. Palacín, *Chem. Mater.*, 2011, **23**, 4109.
15 G. Rousse, M. E. Arroyo-de Domablo, P. Senguttuvan, A. Ponrouch, J. M. Tarascon and M. R. Palacín, *Chem. Mater.*, 2013, **25**, 4946.
16 S. Lee, Y. Cho, H. K. Song, K. T. Lee and J. Cho, *Angew. Chem., Int. Ed.*, 2012, **51**, 8748.
17 J. Xu, D. H. Lee, R. J. Clement, X. Q. Yu, M. Leskes, A. J. Pell, G. Pintacuda, X. Q. Yang, C. P. Grey and Y. S. Meng, *Chem. Mater.*, 2014, **26**, 1260.
18 M. K. Aydinol, A. F. Kohan, G. Ceder, K. Cho and J. Joannopoulos, *Phys. Rev. B: Condens. Matter Mater. Phys.*, 1997, **56**, 1354.
19 W. Ra, M. Nakayama, W. Cho, M. Wakihara and Y. Uchimoto, *Phys. Chem. Chem. Phys.*, 2006, **8**, 882.
20 Y. Shiro, F. Sato, T. Suzuki, T. Iizuka, T. Matsushita and H. Oyanagi, *J. Am. Chem. Soc.*, 1990, **112**, 2921.
21 M. Venkateswarlu, C. H. Chen, J. S. Do, C. W. Lin, T. C. Chou and B. J. Hwang, *J. Power Sources*, 2005, **146**, 204; W. Ra, M. Nakayama, H. Ikuta, Y. Uchimoto and M. Wakihara, *Appl. Phys. Lett.*, 2004, **84**, 4364.